Control of a Grid-Connected Photovoltaic System Based on MPPT and Vector Control

Noureddine Ech-Cherki, Youssef Errami, Abdellatif Obbadi, Smail Sahnoun and Ilham Nassar-Eddine

July 20, 2023

Control of a grid-connected photovoltaic system based on MPPT and vector control

Noureddine Ech-Cherki, Youssef Errami, Abdellatif Obbadi, Smail Sahnoun, Ilham Nassar-Eddine

Laboratory: Electronics, Instrumentation and Energy-Faculty of Science
University Chouaib Doukkali, EL Jadida, Morocco
cherki.ucd@gmail.com

Abstract. This paper describes the control of a Photovoltaic Generator (PVG) connected to the electrical grid. The proposed system is coupled to the electrical grid via two power electronic converters. It consists of a field of solar panels, a DC-DC converter and a three-phase voltage inverter connected to the grid. Current Vector Control (CVC) is proposed to compensate a reactive power injected into the grid and to ensure Maximum Power Point Tracking (MPPT) using global Perturbation and Observation (P&O) method. The performance of the applied technique has been demonstrated under variations of irradiation and temperature.

Keywords: Photovoltaic system, Current vector control, electrical Grid, MPPT, Two conversion stages.

1 Introduction

Today, a large proportion of the world's energy is produced from fossil fuels. Consumption of these sources leads to greenhouse gas emissions and climate pollution. There is a further danger that excessive depletion of natural resource stocks will reduce the energy supply in a way that is dangerous for future generations. Renewable energies present a great opportunity. They are inexhaustible, so we can exploit them more and more easily [1]. Even if certain technologies remain costly. Techniques for extracting maximum power require further research and development to lower installation costs and increase energy performance [2].

Numerous MPPT methods have been developed to improve the energy production capacity of Photovoltaic (PV) systems. These include the P&O method, the Fuzzy Logic method (FL) and the Conductance Increment method (INC). P&O and INC are the most frequently used search algorithms. P&O is an iterative online MPPT method, which uses the PVG module voltage as a disturbance. The INC method is based on the fact that the PV panel's power output is derived from its voltage. To improve energy performance, hybrid methods are used. In [5] a Fractional Open-Circuit Voltage (FOCV) and P&O method are proposed to optimize the duty cycle. In [6], a current-based sliding-mode MPPT algorithm is presented to optimize P&O. In [7], an evaluation has been conducted, comparing the classification and performance of six prominent MPPT techniques that are based on artificial intelligence. In [8], a new modified MPPT algorithm based on P&O and using an adaptive duty cycle step with a genetic algorithm based Proportional, Integral, Derivative (PID) controller is proposed to define the exact MPP. On the other hand, fast dynamic response and robustness are some of the advantages of CVC. Because of these advantages, CVC is used in many studies for the control of power electronic converters. In [9], CVC is employed to transfer energy from the PV system to the grid. In [10] a two-level cascaded inverter is studied using CVC to provide maximum output power and compensate for reactive power.

This paper examines the performance of a photovoltaic system connected to the electrical grid. This system is a combination of a PVG connected to a DC-DC converter, an DC-AC converter and a filter whose task is to eliminate the disturbances present in this grid [3]. Although PVGs are not very cost-effective, MPPT methods and the control of DC-DC and DC-AC converters are capable of operating the PVG at its maximum power. The proposed CVC is one of the popular methods in terms of dynamic responses [4].

This paper is organized as follows. Section 2 presents modeling of system. Section 3 depicts control of system using CVC. The results of the simulation are presented in Section 4. Finally, the conclusion is presented in Section 5.

2 Modelling of system

The system consists of a PVG, a boost converter and a three-phase DC-AC inverter connected to the electrical grid (Fig.1). The boost is used to ensure MPPT approach and the inverter guarantees the control of the power injected into the electrical grid.

2.1 Modeling of the photovoltaic generator

For our application, a 100kW PVG composed of 328 'SunPower SPR-305-WHT' monocrystalline modules. These modules are composed of 66 PV strings connected in parallel, each PV string consisting of 5 PV modules connected in series. A single diode equivalent circuit is applied to study characteristics of this module (Fig.2).

Where V_{pv} and I_{pv} are respectively the voltage and current generated by the PV cell. The equation describing the current and voltage of a solar cell is:

$$I_{pv} = I_{ph} - I_0 \left[\exp\left(\frac{q}{a.k.T} \left(V_{pv} + I_{pv}.R_s \right) \right) - 1 \right] - \frac{V_{pv} + I_{pv}.R_s}{R_{sh}} \quad (1)$$

where I_{ph} is the photocurrent proportional to solar irradiation of the cell; I_0 is the saturation current, q: electronic charge, k: Boltzmann constant, α is the solar cell ideality factor; R_s is the series resistance and R_{sh} is the shunt resistance. To obtain a mathematical model of a PVG, all losses caused by the combination of modules in series and in parallel are included, giving the equation (2):

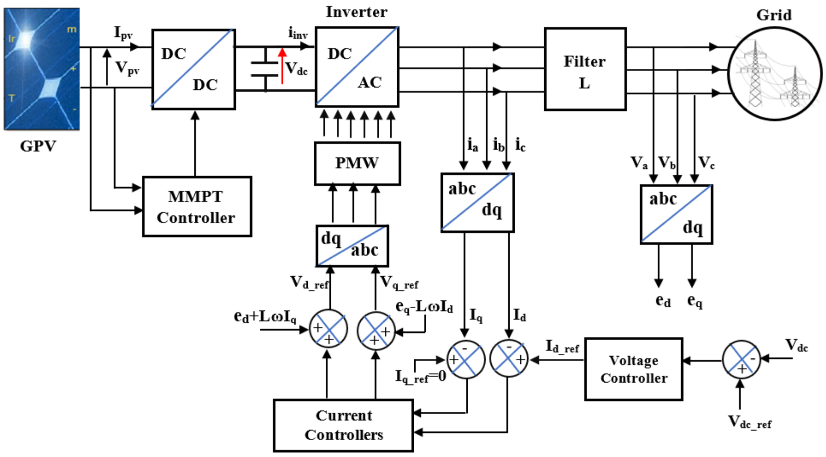

Fig. 1. Topology of a photovoltaic system connected to the electrical grid

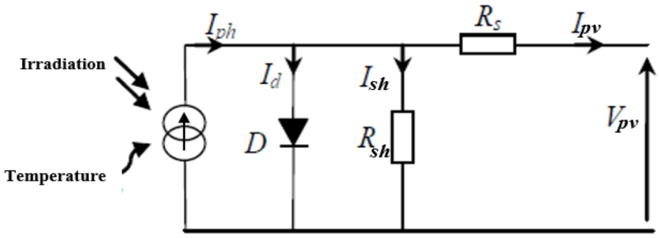

Fig. 2. Equivalent circuit of a single diode PV cell

$$I_{pv} = N_p.I_{ph} - N_p.\, I_0\left[\exp\left(\frac{q}{\alpha.k.T}\left(\frac{V_{pv}}{N_s}+\frac{I_{pv}.R_s}{N_p}\right)\right)-1\right]-\frac{N_p}{R_{sh}}\left(\frac{V_{pv}}{N_s}+\frac{I_{pv}.R_s}{N_p}\right) \qquad (2)$$

Where N_p and N_s are respectively the number of modules connected in parallel and in series. In this paper, a generalized five-parameter model is simulated using the MATLAB/Simulink software environment. We used the parameter identification methods from [11]. The Fig.3 shows the PVG's P(V) characteristics as a function of irradiation Fig.3 (a) and temperature Fig.3 (b). We find that the PVG's output characteristics are non-linear, and the power is strongly affected by solar radiation. To keep the PVG running at MPP, an MPPT controller is used to control the DC-DC converter.

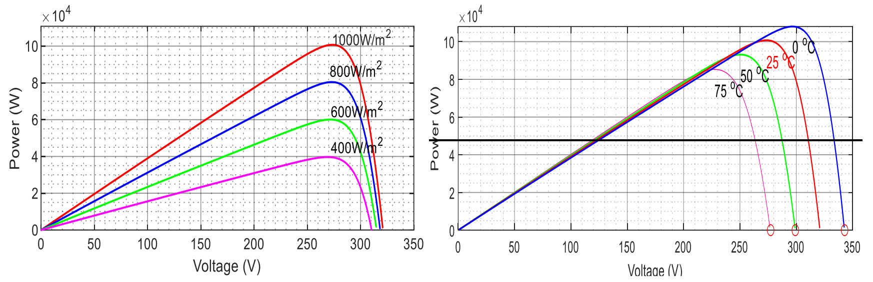

(a) ***(b)***

Fig. 3. PVG characteristics as a function of irradiation (a) and temperature (b)

2.2 DC-DC boost converter

The DC-DC boost converter is used as an interface to adapt the voltage between the PVG and the inverter. Its output voltage can be expressed as follows:

$$\frac{V_{dc}}{V_{pv}} = \frac{1}{1-\alpha} \tag{3}$$

where α is the duty cycle controlled by the algorithm P&O to maintain the optimal voltage V_{pv} which guarantees a maximum power of the PVG. V_{dc} is the voltage between the boost and the inverter that which regulated by PI regulator. The DC bus reference voltage is calculated using the next equation [12].

$$V_{dc\_ref} = \frac{2\sqrt{2}\,.\,V_{LL}}{\sqrt{3}.\,m_a} \tag{4}$$

where "V_{LL}" is the line-to-line network voltage, "m_a" is the modulation index. The DC bus voltage is accepted as 700 V (m_a=1 and V_{LL} = 381 V).

2.3 Three-phase DC-AC inverter

The DC-AC converter is a two-level, three-phase voltage source inverter controlled by the Pulse Width Modulation (PWM) strategy. It is connected to the three-phase electrical grid via an 'L' inductive filter. The dynamic equations of the link with the inductive filter and the grid, in the park reference, are described by:

$$\begin{cases} L_f.\dfrac{di_d}{dt} = -R.i_d + L_f w i_q + V_d - e_d \\ L_f.\dfrac{di_q}{dt} = -R.i_q - L_f w i_d + V_q - e_q \end{cases} \tag{5}$$

With ω is the grid pulsation (ω=2πf$_r$), i_d and i_q are the direct and quadrature components of the current, V_d and e_d are the direct components of the voltage on the inverter and grid side while V_q and e_q are its quadrature components. L_f is the inductance of the inverter-grid coupling filter and R_f is the damping resistance of the filter. The smoothing inductance is given by the next equation [12]:

$$L_f = \frac{V_{dc}}{6.\, f_{sw} \,.\, \Delta_{ph\text{-}max}} \quad (6)$$

Where $\Delta_{ph\text{-}max}$ the variation in peak current ripple, in this work $\Delta_{ph\text{-}max}$ = 10%, and "F_{sw}" is the system switching frequency.

3 Photovoltaic system control

3.1 MPPT control

In this work, we used a classical P&O control. Its principle is based on perturbing the system by increasing or decreasing voltage, then observing the effect on output power in order to correct the duty cycle [5].

3.2 Control of DC bus voltage

The inverter is utilized to keep DC link voltage constant and equal to its reference (V_{dc}=$V_{dc\text{-}ref}$ =700V) [13]. The current in the capacitor is given by:

$$i_{dc} = C_{bus} . \frac{dV_{bus}}{dt} = i_L - i_{inv} \quad (7)$$

We can then regulate the DC bus voltage by controlling the inverter current i_{inv} with a PI controller. The PI controller parameters are derived by comparing the system's closed cycle transfer function with the transfer function of the second order system:

$$\begin{cases} k_i = C.\, \omega_n^2 \\ k_p = 2.\xi.\, C.\, \omega_n \end{cases} \quad (8)$$

Where ω_n is the natural pulsation and ξ=0.707 is the damping coefficient.

3.3 Control of inverter on grid side

The objective of inverter control on the grid side is to regulate active (P) and reactive (Q) power using CVC [1]. The PI controller parameters are derived by comparing the system's closed cycle transfer function with the transfer function of the second order system:

$$\begin{cases} k_i = L_f \,.\, \omega_n^2 \\ k_p = 2.\xi.\, L.\, \omega_n - R \end{cases} \quad (9)$$

The orientation of the rotating reference frame is used to obtain separate control of P and Q. So, V_d = V and V_q =0. The expression for active power P and reactive power Q in the Park domain is given by [13]:

$$\begin{cases} P = \frac{3}{2}\left(V_d . i_d\right) \\ Q = -\frac{3}{2}\left(V_d . i_q\right) \end{cases} \tag{10}$$

Consequently, to control the direct i_d and quadrature i_q components of the current and consequently the active and reactive power, we need to eliminate the coupling terms and compensate for the mains voltage components (e_d and e_q). The two PI controllers compare the reference currents ($i_{d\text{-}ref}$ and $i_{q\text{-}ref}$) with the inverter output currents (i_d and i_q).

$$\begin{cases} V_{d\_ref} = \left(k_p + \frac{k_i}{p}\right).\left(i_{d\_ref} - i_d\right) + e_d - L\omega i_q \\ V_{q\_ref} = \left(k_p + \frac{k_i}{p}\right).\left(i_{q\_ref} - i_q\right) + e_q + L\omega i_d \end{cases} \tag{11}$$

So, we control V_{d_ref} and V_{q_ref} by controlling currents i_d and i_q to make the necessary corrections to obtain a zero static error. Fig. 1 illustrates the configuration of the control system.

4 Results of simulations

The power flow control performance of the proposed algorithms has been evaluated under varying irradiation conditions. The irradiation curve is shown in Fig.4. The PV power results are given in Fig.5. As shown in the figure, the MPPT algorithm follows the point at maximum power with success ($P_{\_MPP}$=100kW at 1kW/m^2). The results of PVG current and DC bus voltage V_{dc} are given in Fig. 6 and Fig. 7 respectively, While the current increases up to 368.3A (equal to the PVG current at 1kW/m^2) and the voltage value V_{dc} is successfully fixed at the reference (V_{dc_ref}=700V). In Fig.8 the inverter currents are successfully fixed at the reference value (i_{ref}). Since the MPPT algorithm changes the value of the reference current, the output currents of the inverter are also changed according to the irradiance curve in Fig.4.The performance of the system with CVC is shown in Fig. 8 and Fig.9. It can be seen from these figures, that after the initial transients, the system achieves stable operational states. Voltage and current are in phase (Fig.8). The system achieves the unit power factor operation (Fig.9).

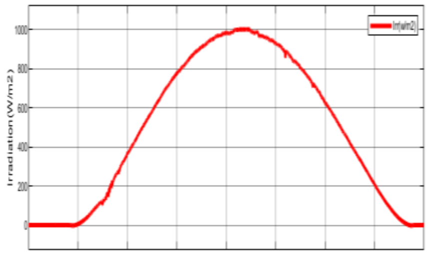

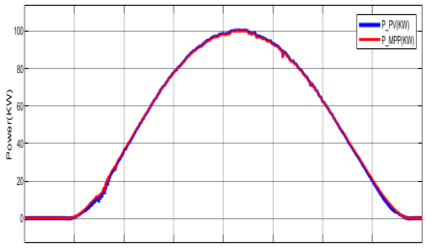

Fig .4. Irradiation curve **Fig.5**. PV power results

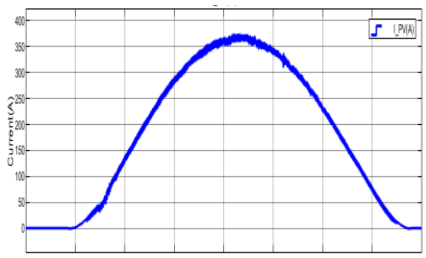

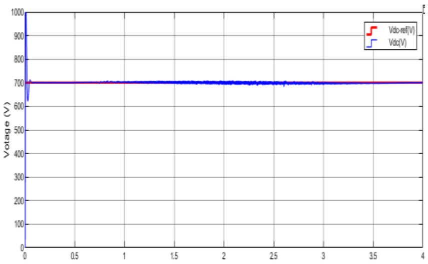

Fig.6: Results of PVG current **Fig.7:** Results of V_{dc} voltage

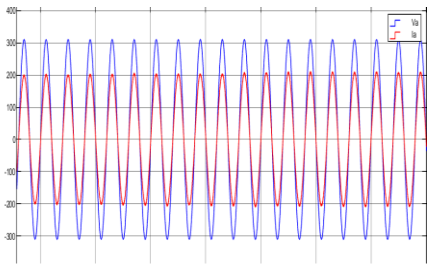

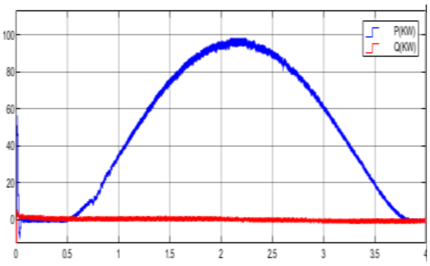

Fig. 8: Grid current and voltage **Fig. 9:** Active and reactive power

Table 1. system parameters

Parameter	**Symbol**	**Value**
DC bus capacitor	C	2000µF
Inductance of the inverter-grid coupling	L_f	3.6mH
Inverter switching frequency	F_{sw}	5kHz
Integral gain of current PI controllers	K_i	60
Proportional gain of current PI controllers	K_p	20.8
Integral gain of the DC bus PI controller	K_i	75
Proportional gain of the DC bus PI controller	K_p	0.51

5 Conclusion

This paper discusses the optimal control of a grid connected photovoltaic system and optimizes MPPT tracking performance. An MPPT method based on the P&O algorithm for the PVG, and a strategy based on current vector control for the inverter are proposed. The steady-state and dynamic performances of the system are verified by simulation under different irradiation and temperature values. When these factors change, the P&O controller quickly tracks the PVG's maximum power point, and the electrical grid connected PV system produces stable active power.

References

1. A. Jemmali, H. Abid, K. Elleuch and A. Toumi, "Control Structure for a Photovoltaic Chain Connected to the Three-phase Grid," 2020 17th International Multi-Conference on Systems, Signals & Devices (SSD), Monastir, Tunisia, 2020, pp. 525-529.
2. Ahmed, Mostafa, Mohamed Abdelrahem, and Ralph Kennel. "Highly efficient and robust grid connected photovoltaic system-based model predictive control with kalman filtering capability." Sustainability 12.11 (2020).
3. Zhao, Y., An, A., Xu, Y. et al. Model predictive control of grid-connected PV power generation system considering optimal MPPT control of PV modules. Prot Control Mod Power Syst 6, 32 (2021).
4. N. Güler and E. Irmak, "MPPT Based Model Predictive Control of Grid Connected Inverter for PV Systems," 2019 8th International Conference on Renewable Energy Research and Applications (ICRERA), Brasov, Romania, 2019, pp. 982-986.
5. Suresh Srinivasan, Ramji Tiwari, Murugaperumal Krishnamoorthy, M.Padma Lalitha, K.Kalyan Raj,Neural network based MPPT control with reconfigured quadratic boost converter for fuel cell application,International Journal of Hydrogen Energy,Volume 46, Issue 9,2021,Pages 6709-6719,
6. Haq, Izhar Ul, et al. "Neural network-based adaptive global sliding mode MPPT controller design for stand-alone photovoltaic systems." Plos one 17.1 (2022).
7. KY Yap, CR Sarimuthu et JM-Y. Lim, "Techniques MPPT basées sur l'intelligence artificielle pour le système d'alimentation solaire : une revue", dans Journal of Modern Power Systems and Clean Energy, vol. 8, non. 6, pp. 1043-1059, novembre 2020.
8. A. Harrag, S. Messalti, Variable step size modified P&O MPPT algorithm using GA-based hybrid offline/online PID controller, Renew. Sustain. Energy Rev. 49(2015) 1247–1260
9. Mahamat, Chabakata. "Analysis and controls of multi-level converters for a grid connected photovoltaic system." (2018).
10. Benbouhenni, Habib. "Comparison study between seven-level SVPWM and two-level SVPWM strategy in direct vector control of a DFIG-based wind energy conversion systems." International Journal of Applied Power Engineering (IJAPE) 9.1 (2020): 12-21.
11. I. Nassar-eddine, A. Obbadi, Y. Errami, A. El fajri, M. Agunaou, Parameter estimation of photovoltaic modules using iterative method and the Lambert W function: Comparative study, Energy Conversion and Management, Volume 119,2016, Pages 37-48.
12. Özgür, C., and A. Teke. "A hybrid MPPT method for grid connected photovoltaic systems under rapidly changing atmospheric and Technology." Electric Power Systems Research 152 (2017): 194-210.
13. S. Sok, "Study on Grid-Connected Inverter with Gigantic Utility Impedance Vacillation by Using LCL Filter," 2023 8th Asia Conference on Power and Electrical Engineering (ACPEE), Tianjin, China, 2023, pp. 1492-1497.